Phosphorylation of the Major *Drosophila* Lamin In Vivo: Site Identification during Both M-Phase (Meiosis) and Interphase by Electrospray Ionization Tandem Mass Spectrometry†

Ulrich Schneider,‡ Thierry Mini,‡ Paul Jenö,*,‡ Paul A. Fisher,§ and Nico Stuurman||

Department of Biochemistry, Biozentrum of the University of Basel, CH-4056 Basel, Switzerland, Department of Pharmacological Sciences, Health Sciences Center, SUNY at Stony Brook, Stony Brook, New York 11794-8651, and The Maurice E. Müller Institut at the Biozentrum of the University of Basel, CH-4056 Basel, Switzerland

Received November 12, 1998; Revised Manuscript Received January 29, 1999

ABSTRACT: Phosphorylation can have profound effects on the properties of nuclear lamins. For instance, phosphorylation of specific sites on mammalian lamins drastically alters their propensity to polymerize. Relatively little is known about the effects of phosphorylation during interphase and about phosphorylation of invertebrate nuclear lamins. Here, using electrospray ionization tandem mass spectrometry, we determined the phosphorylation sites of both interphase and M-phase isoforms of nuclear lamin Dm from *Drosophila melanogaster*. Interphase lamins are phosphorylated at three sites: two of these sites (Ser_{25} and a site located between residues 430 and 438) flank the α-helical rod domain, whereas the third site (Ser_{595}) is located close to the C-terminus. The M-phase lamin isoform is phosphorylated predominantly at Ser_{45}, a residue contained within a sequence matching the consensus site for phosphorylation by cdc2 kinase. Our study confirms the important role in vivo for cdc2 kinase in M-phase disassembly of nuclear lamins and provides the basis for understanding *Drosophila* lamin phosphorylation during interphase.

It is increasingly appreciated that structural aspects of the cell nucleus play important roles in the regulation of gene expression (*1*). The general rules that govern nuclear structure are still elusive, but insights are likely to be found in the study of nuclear proteins that can (self-) polymerize, a property common to the basic elements of the cytoskeleton. Nuclear lamins are the only known members of the family of intermediate filament proteins located in the cell nucleus (*2*). Nuclear lamins self-assemble in vitro and form a network underlying the inner nuclear membrane in vivo (*3*). In addition, nuclear lamins can be found in various forms in the nuclear interior (*4*, *5*). Lamins are thought to help protect the nucleus from mechanical distortions (*6*), they arrange nuclear pore complexes spatially (*3*, *7*), they might be involved in organizing chromatin (*8*−*10*), and they play a role in DNA replication (*11*).

Nuclear lamins, like other intermediate filament proteins, contain a central α-helical rod domain which is essential in the generation of parallel, unstaggered dimers through coiled-coil formation (*2*). Lamins also contain relatively short N-terminal heads and longer C-terminal tails whose structures are not well-known (*11*, *12*). Lamin dimers can line up longitudinally to form head-to-tail polymers (*13*, *14*). Assembly of lamins in vivo likely depends on this longitudinal interaction as well as lateral interactions between lamin dimers (*3*).

Disassembly of the nuclear lamina during mitosis is accompanied by lamin phosphorylation (*15*, *16*). There is considerable evidence that cdc2 kinase (the p34cdc2-cyclin B complex) is instrumental in M-phase lamin phosphorylation and disassembly (*17*−*23*). In addition, M-phase breakdown of the nuclear lamina can be induced by protein kinase C (PKC) (*24*−*27*). These findings suggest that various kinases can disassemble nuclear lamins and that different cell types may use different enzymes.

Nuclear lamins are also phosphorylated during interphase (*15*). Not much is known about the function of interphase lamin phosphorylation. However, phosphorylation of chicken lamin B_2 by PKC at a site close to the nuclear localization signal inhibits import of lamin into the cell nucleus (*28*). An unidentified site in human lamin B_2 is phosphorylated specifically during S-phase (*29*).

The invertebrate *Drosophila melanogaster* contains at least two lamin genes. The expression of one of these, called lamin C (*30*), is developmentally regulated, whereas the lamin Dm_0 gene is expressed in all cell types except for mature sperm (*31*−*33*). Unless indicated otherwise, for *Drosophila*, the term lamin refers solely to protein products encoded by the *Drosophila* lamin Dm_0 gene.

We purified two lamin isoforms from *Drosophila* embryos. Large stores of maternal mRNA as well as protein are deposited into the *Drosophila* oocyte for use later in development. From oocyte stage 6 to 7 onward, the lamin

† Supported by the Swiss National Research Foundation Grant 3100-049416.96/1 (U.S.), the U.S. NIH Grant GM33132 (P.A.F.), and a Long-Term Fellowship from EMBO (N.S.).

* To whom correspondence should be addressed at the Department of Biochemistry, Biozentrum of the University of Basel, Klingelbergstrasse 70, CH-4056 Basel, Switzerland. Phone: +41 61 267 21 68. Fax: +41 61 267 21 48. E-mail jenoe@ubaclu.unibas.ch.

‡ Biozentrum of the University of Basel, Switzerland.

§ SUNY at Stony Brook, Stony Brook, NY.

|| The Maurice E. Müller Institut at the Biozentrum of the University of Basel, Switzerland.

10.1021/bi9827060 CCC: $18.00
Published on Web 03/18/1999

protein accumulates as a soluble species in the cytoplasm as well as in the nucleus of the developing oocyte (*33*, *34*). After fertilization, a number of rapid nuclear divisions take place within a syncytium. Lamin purified from such early embryos is soluble, migrates on SDS-polyacrylamide gels as a single 75 kDa species, has many similarities with lamin purified from mitotic *Drosophila* tissue culture cells, and was called lamin Dm_{mit}. During later stages of embryonic development, most lamin is associated with nuclei, and, when purified, appears as two bands with apparent molecular masses of 74 kDa (Dm_1) and 76 kDa (Dm_2) on SDS-polyacrylamide gels (*34*, *35*). Lamin Dm_{mit} and interphase lamins Dm_1 and Dm_2 contain similar amounts of phosphate per molecule of protein. However, whereas lamin Dm_{mit} contains exclusively phosphoserine, lamins Dm_1 and Dm_2 are phosphorylated on both serine and threonine (*34*), demonstrating that interphase and M-phase lamins are phosphorylated on different sites.

To understand the function of lamin phosphorylation it is essential to know which residues are phosphorylated. We therefore set out to investigate the sites of phosphorylation in lamin Dm_1/Dm_2 and Dm_{mit}. With a combination of enzymatic mapping and electrospray ionization tandem mass spectrometry, we observed that interphase lamin phosphorylation occurs on three distinct portions of the protein: at segments of the head and tail domains that flank the α-helical rod domain as well as at the very C-terminal end of the tail domain preceding the CaaX box. These three sites are not phosphorylated in M-phase lamin. Instead, a new site lying close the N-terminal end of the rod domain with a typical consensus sequence for cdc2 kinase is phosphorylated in this isoform.

MATERIALS AND METHODS

Preparation of Interphase and M-Phase Lamin. Interphase lamin was prepared from 6−18 h old *Drosophila* (Canton-S strain) embryos (*36*). Typically, 6−7 mL of packed embryos (corresponding to 250 000−350 000 organisms) were processed in each preparation. Final purification of lamin was achieved by passing the nuclear extract over a column (1 × 5 cm) packed with Sepharose beads to which antilamin antibodies had been coupled covalently. Lamin was eluted from the antibody support with 50 mM glycine buffered to pH 2.3, containing 500 mM NaCl and 0.1% Triton X-100, and the lamin containing fractions were pooled. The detergent was removed by diluting the salt concentration of the lamin pool to below 100 mM NaCl, and polymerized lamin was pelleted at 10 000 rpm for 15 min in an Eppendorf centrifuge. The precipitate was washed three times with 25 mM MOPS, pH 7.0. The final pellet was dissolved in 50 μL 25 mM MOPS, pH 7.0, containing 6 M urea to yield a protein concentration of 1−2 μg/μL.

Soluble lamin Dm_{mit} from 0−4 h old *Drosophila melanogaster* embryos was isolated by affinity chromatography as described above (*35*, *36*). Pooled fractions from the antibody column were first concentrated by TCA[1]−deoxycholate precipitation before redissolving the protein in 50 μL 50 mM MOPS, pH 7.0, containing 6 M urea. For removal of detergent, the protein was precipitated with ethanol and the pellet was washed extensively with acetone. The pellet was redissolved in 50 μL 50 mM MOPS, pH 7.0, containing 6 M urea to yield a protein concentration of 1−2 μg/μL. All lamin preparations were stored at −20 °C until further use.

Enzymatic Digestions. Lamin was digested with endoproteinase LysC (*Achromobacter* Protease I, Wako Chemicals) at an enzyme/substrate ratio of 1:50 at 37 °C for 1 h in 100 mM Tris-HCl, pH 8.0, containing 6 M urea. The reaction was stopped by adding TFA from a 4% stock solution to a final concentration of 0.2%, and the digest was analyzed either by capillary LC/MS or the endoproteinase LysC peptides were isolated preparatively on a C_{18} microbore column. Double digestions of lamin with endoproteinase LysC and trypsin (sequencing grade, Boehringer, Mannheim) were carried out by incubating the protein with the endoproteinase LysC as described above. Before addition of trypsin, the urea concentration was lowered to 2 M by adding 100 mM Tris-HCl, pH 8.0, and incubation was continued at 37 °C for 2 h at a trypsin/substrate ratio of 1:20. Endoproteinase LysC peptides of lamin which had been isolated by microbore RP HPLC were neutralized with a minimal volume of Tris base before addition of the enzyme. Tryptic and chymotryptic (sequencing grade, Boehringer, Mannheim) digestions were with 50−100 ng enzyme for 1 h at 37 °C. Clostripain digestions were with 1 μg enzyme (from *Clostridium histolyticum*, Boehringer, Mannheim). Prior to use, clostripain was activated at room temperature with 2.5 mM DTT in 50 mM Tris-HCl, pH8.0, 50 mM $CaCl_2$ for 1 h (*37*). All reactions were stopped by acidification with 10% TFA to a final concentration of 0.5% before analyzing them by capillary LC/MS.

Peptide and Ion Nomenclature. Peptides generated by endoproteinase LysC are labeled with K, peptides obtained by tryptic cleavage are marked with T, and peptides generated by clostripain cleavage are denoted with CP. The peptides are numbered sequentially according to their position based on the *Drosophila melanogaster* sequence (*36*, *38*). In numbering specific residues of the lamin sequence, it is assumed that the sequence starts with the methionine at position 1. Peptides selected for fragmentation in the collision cell of the mass spectrometer are labeled in the corresponding figures by $[M + nH]^{n+}$, where *n* represents the number of protons attached to the peptide. To avoid confusion between numbering of y- and b-ions generated during collision-induced fragmentation and residue numbering of amino acids, the starting and ending residues of each fragment are indicated in the corresponding figures.

Mass Spectral Analyses. The microspray needles used for electrospray ionization were pulled from 100 μm i.d. × 280 μm o.d. fused silica capillaries (LC Packings, Amsterdam, The Netherlands) on a model P-2000 quartz micropipette puller (Sutter Instrument Company, Novato, CA). For LC/MS analysis, the needles were placed into an XYZ micropositioner and the voltage was applied directly to the sample stream through the capillary union (*39*). Spray voltages were usually between 1100 and 1400V. Mass determinations were carried out on a TSQ7000 triple quadrupole mass spectrometer (Finnigan, San José, CA). All measurements were carried out in the positive ion mode. For operation in the MS/MS

[1] Abbreviations: CID, collision-induced dissociation; LC/MS, liquid chromatography−mass spectrometry; MS/MS, tandem mass spectrometry; *m*/*z*, mass-to-charge ratio; RP HPLC, reverse-phase high-performance liquid chromatography; TCA, trichloroacetic acid; TFA, trifluoroacetic acid.

Table 1: Calculated and Measured Masses of the Endoproteinase LysC Peptides of Interphase *Drosophila* Lamin[a]

peptide	residues	scan no.	calcd mass (Da)	measured mass (Da)
K_1	1−4		452.2	
K_2/K_2*	5−55	382	5222.7	5222.7/5303.1*
K_3	56−101	691	5431.9	5431.1
K_4	102−130	697	3442.8	3443.0
K_5	131−140		1372.7	
K_6	141−142		261.2	
K_7	143−145		375.2	
K_8	146−146		147.1	
K_9	147−148		248.2	
K_{10}	149−170	462	2529.2	5060.7[b]
K_{11}	171−179	184	1079.5	1079.1
K_{12}	180−180		147.1	
K_{13}	181−190	380	1158.6	1158.5
K_{14}	191−197	279	943.6	943.1
K_{15}	198−204	215	937.5	937.1
K_{16}	205−230	736	3091.6	3089.9
K_{17}	231−245	325	1853.0	1852.8
K_{18}	246−263	432	2091.0	2091.2
K_{19}	264−265		260.2	
K_{20}	266−293		3406.7	
K_{21}	294−310	313	1911.0	1910.7
K_{22}	311−366	749	6580.4	6579.0
K_{23}	367−380	493	1787.0	1786.8
K_{24}	381−389	430	1154.5	1154.2
K_{25}	390−401	522	1336.7	1336.7
K_{26}/K_{26}*	402−446	577	4797.6	4797.5/4878.1*
K_{27}	447−448		303.2	
K_{28}	449−470	418	2398.1	2397.4
K_{29}	471−476	210	659.4	659.0
K_{30}	477−483	215	787.4	786.6
K_{31}	484−490	423	923.6	922.9
K_{32}	491−509	588	2127.1	2127.0
K_{33}	510−516	189	753.4	752.6
K_{34}	517−537	526	2412.3	2412.3
K_{35}	538−549	347	1282.7	1282.8
K_{36}	550−552		362.2	
K_{37}	553−578	631	2885.5	2885.3
K_{38}/K_{38}*	579−618	392	4579.3	4577.4/4658.0*
K_{39}	619−622		437.2	

[a] The elution position of the peptides is denoted by the corresponding scan number (each scan is 3 seconds). Blank cells indicate peptides which were not observed during the LC/MS analysis. Peptides found to be phosphorylated are marked with an asterisk and the masses of the nonphosphorylated and phosphorylated peptides are shown. [b] K_{10} was found to be dimerized.

mode, the resolution of Q1 was set to transmit a mass window of 4 Da and resolution of Q3 was adjusted to 1.5 Da. Scanning was performed between 50 and 2250 Da in 3.5 s. Argon was used as collision gas at a pressure of 3.5 mTorr. MS/MS spectra were acquired by injecting peptides onto a 100 μm i.d. capillary column packed with POROS R2 (20 μm particle size, 3−5 cm in length). Peptides were desorbed into the mass spectrometer with a 10 min gradient consisting of 0−80% acetonitrile in 0.02% acetic acid at flow rates of 100−200 nL/min. The collision energy was individually tuned for each peptide to optimize the quality of the collision spectra.

RESULTS

Identification of Phosphopeptides. To identify phosphorylation sites, lamin was digested with endoproteinase LysC and the masses of the resulting peptides were analyzed by LC/MS and compared to the predicted masses, on the basis of the specificity of the proteinase. Phosphopeptides were identified by screening for peptides whose masses are 80 Da higher (or multiples thereof if multiple sites on a single peptide are phosphorylated) than the predicted mass. Twenty seven peptides were observed in the LC/MS analysis of the endoproteinase LysC digest of lamin isolated from 6−18 h old embryos (henceforth called interphase lamin) (Table 1). These peptides accounted for 93 out of a total of 99 Ser/Thr residues in the lamin sequence (Tyr phosphorylation of *Drosophila* lamin has not been observed (*34*)).

Examining the spectra for the presence of peptides whose masses are increased by 80 Da (or multiples thereof), three candidates were found: the peptide K_2, which precedes the α-helical rod domain, K_{26}, located just after the α-helical rod domain, and K_{38} which precedes the carboxyl-terminal CaaX box (Figure 1). The signals of each of these peptide ions were accompanied by signals with mass increments of 20 and 27 Da for the quadruply and triply charged molecular ions (Figure 2), characteristic of phosphopeptides where the phosphate group adds 80 Da to the mass (or 80 Da/z for multiply charged ions). Assuming no preferential loss of either phosphorylated or unphosphorylated forms of a peptide during chromatography and that phosphorylated and unphosphorylated peptides are ionized with equal efficiencies in the ion source, the ratio of intensities of the signals for the phospho and nonphospho forms of peptides can be taken as a measure for the extent of phosphorylation of these peptides. Comparison of the integrated peak areas of the various charge forms for the three phosphopeptides with the peak areas of the corresponding charge forms of the unphosphorylated peptides in the spectrum recorded from interphase lamin indicates the approximate extent of phosphorylation to be

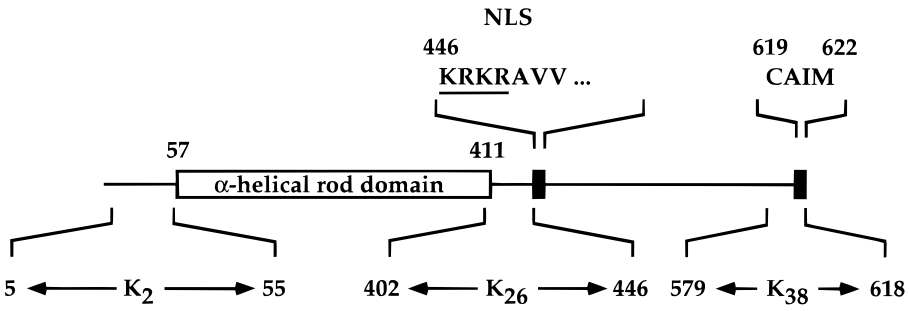

FIGURE 1: Domain structure of *Drosophila* lamin. The N-terminal head and the C-terminal tail domain comprise residues 1−56 and 412−622, respectively, which are separated by the α-helical rod domain (residues 57−411). The nuclear localization signal (NLS) is underlined. The sequence CAIM is a four amino acid stretch at the C-terminus of lamin which gives rise to farnesylation and carboxymethylation of the protein (also called the CaaX box). The peptides labeled K_2, K_{26}, and K_{38} show those peptides produced by endoproteinase LysC digestion which were found to be phosphorylated.

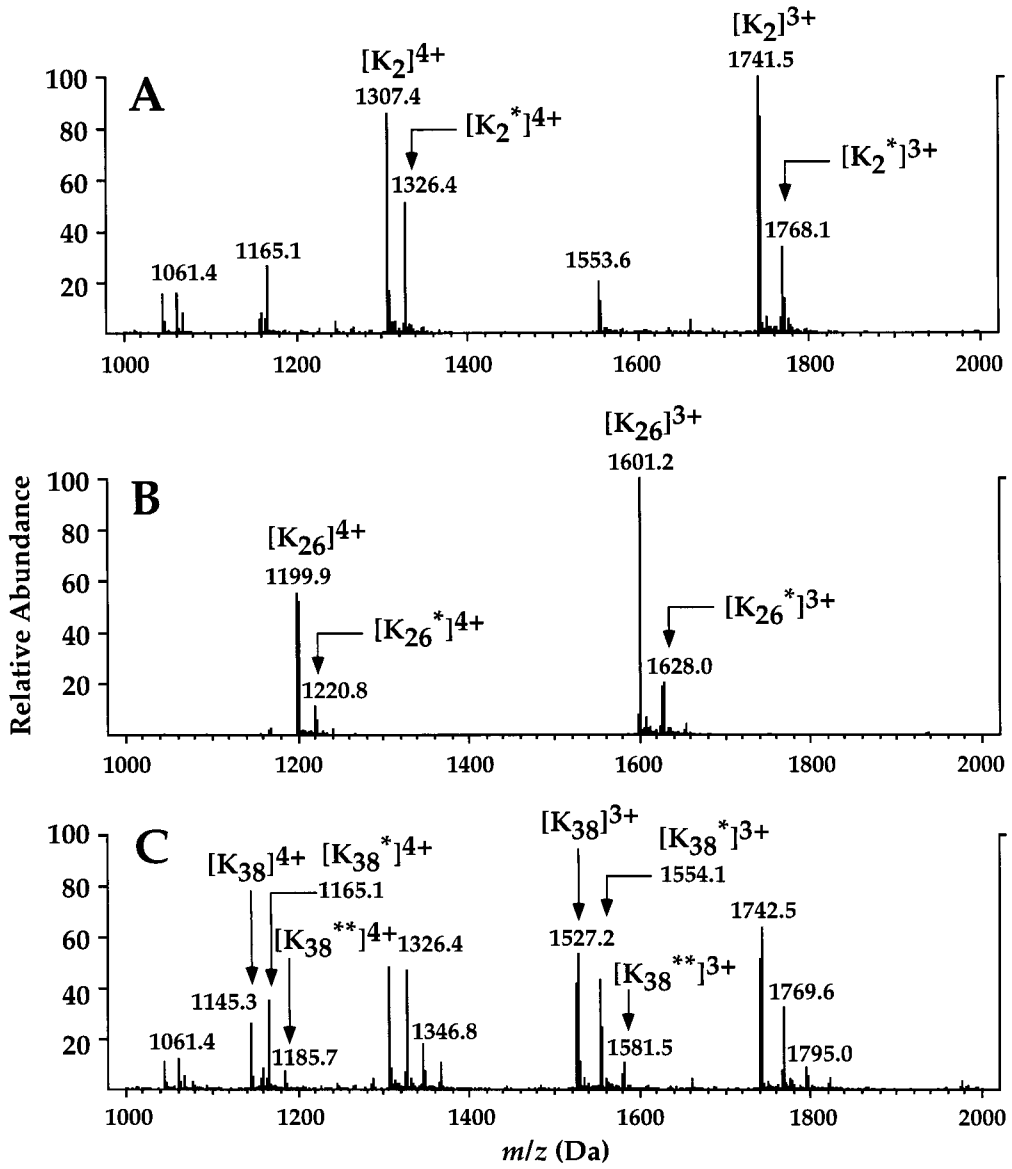

FIGURE 2: Spectrum of the three phosphopeptides K_2 (A), K_{26} (B), and K_{38} (C) from interphase lamin. Because of the large size, each peptide produces a complex spectrum of multiply charged ions. Therefore, for reasons of clarity, only the triply and quadruply charged peptides (labeled with 3+, and 4+, respectively) in the mass range between 1000 and 2000 Da are shown. Singly phosphorylated peptides are labeled with an asterisk, the doubly phosphorylated peptide K_{38} is marked with two asterisks. Because it was not possible to separate all of the lamin peptides into single components during an LC/MS run, the spectrum shown in panel A contains signals from coeluting peptides other than K_2, whereas the spectrum in panel C shows a mixture of coeluting K_{38} and K_2. Signals which are not labeled in the spectrum correspond to coeluting peptides other than K_2, K_{26}, or K_{38}.

23−29% for K_2, 13−19% for K_{26}, and 42−48% for K_{38}. Small amounts of doubly phosphorylated K_{38} are also apparent in the spectrum (Figure 2C), but their low stoichiometry of phosphorylation precluded further analysis. It should be pointed out that the stoichiometry of phosphorylation for the three peptides K_2, K_{26}, and K_{38} deduced from the ion intensites of the unphosphorylated and phosphorylated peptides can only be an approximation. Although it has been shown that the ratio of phosphorylated to unphosphorylated peptides in the full scan positive-ion data can be used to estimate the stoichiometry of phosphorylation (*40*), our observations indicate that the relative areas between phosphorylated and unphosphorylated peptide varies with the charge state (see Figure 2, peptide K_{38}). Therefore, the stoichiometry of phosphorylation for the three peptides deduced in the present study are averaged values from a number of charge states and, accordingly, show a relatively high variation. Nevertheless, large changes in phosphorylation which occur at a given site can still be followed when peak areas from spectra of the corresponding phospho/nonphospho forms are compared (see below).

When the endoproteinase LysC digest of the M-phase form of lamin was chromatographed under the same conditions, all of the peptides mentioned in the table were observed except K_5 and K_{20}. Comparison of the spectra of the three phosphopeptides from interphase and M-phase lamin shows major differences in the stoichiometry of phosphorylation: whereas the degree of phosphorylation for K_{26} and K_{38} is substantially lower in M-phase lamin, phosphorylation of K_2 is approximately threefold higher (Figures 2 and 3).

The three candidate phosphopeptides K_2, K_{26}, and K_{38} contain multiple potential phosphorylation sites. To precisely locate the phosphorylated residues, ions of each individual peptide are selected in the first quadrupole of the mass

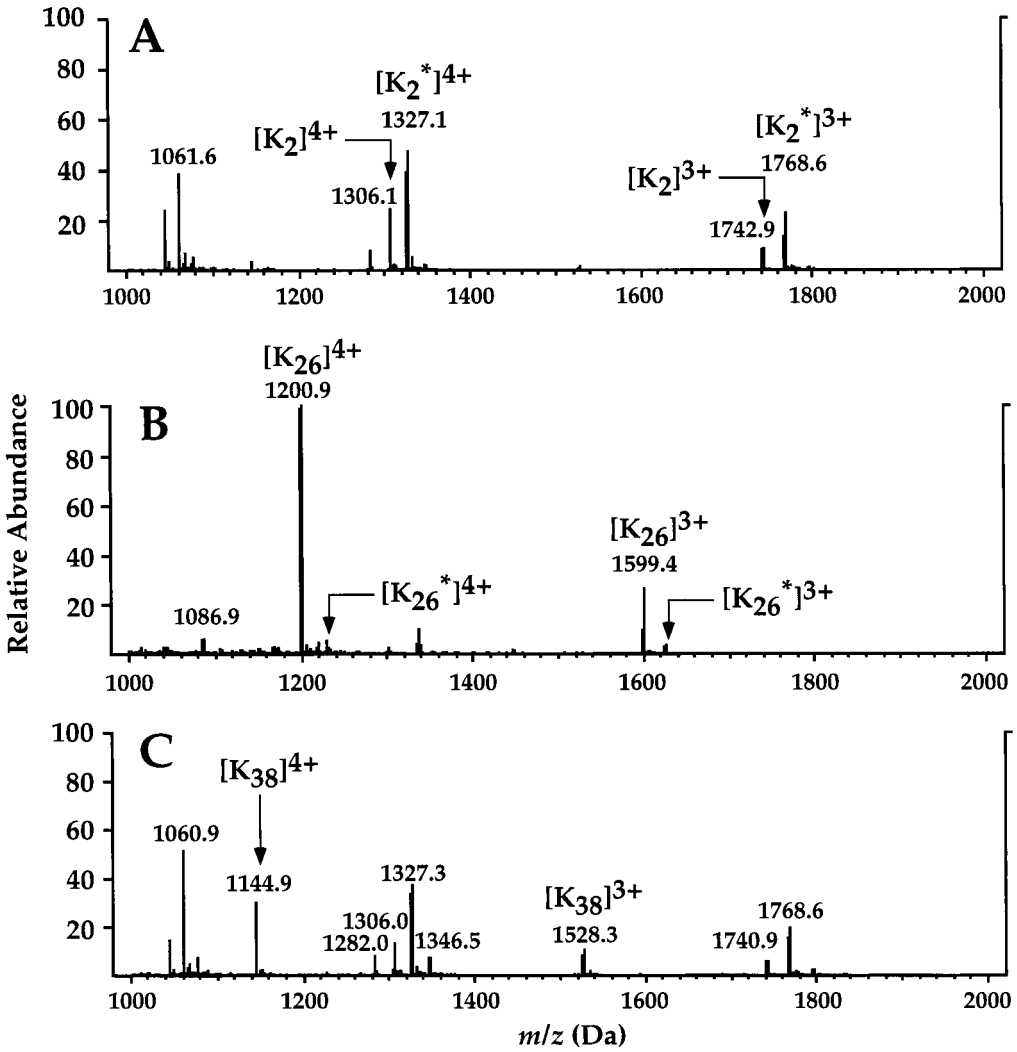

FIGURE 3: Spectrum of K_2 (A), K_{26} (B), and K_{38} (C) from M-phase lamin. For labeling of the peptides see Figure 2.

spectrometer and subjected to fragmentation in a collision cell to produce ions from which the sequence of the peptide can be deduced. When the fragmentation pattern of a phosphopeptide is compared with that of its nonphosphorylated counterpart, a shift of 80 Da (or divided by the corresponding charge state of the fragment ions) can be observed when a phosphorylated residue is encountered. In addition, partial elimination of phosphoric acid (98 Da) upon fragmentation in the collision cell can occur, generating daughter ions separated by 98, 49, and 32.7 Da from parent ions having a charge of +1, +2 and +3 (*41*).

Analysis of Phosphopeptide K_{38} from Interphase Lamin. Initial attempts to determine the site of phosphorylation by subjecting K_{38} from interphase lamin to fragmentation by collision-induced dissociation were not successful because of the large size of the peptide. Therefore, the endoproteinase LysC peptides were further digested with trypsin to obtain smaller peptides. Complete tryptic digestion of K_{38} should produce six cleavage products: three single arginines, and the three peptides T_{94}, T_{95}, and T_{98} (Figure 4A). In an LC/MS analysis of an endoproteinase LysC/tryptic digest of interphase lamin, both phosphorylated and unphosphorylated T_{98} were found in the triply charged form (891.4 and 918.1 Da, respectively, Figure 4B). The N-terminal peptide T_{94} was also detected and eluted between scans 55 and 65. No phosphorylated T_{94} was observed (results not shown). The tripeptide LSR (T_{95}) could not be found, but due to its high polarity, the peptide is not expected to bind to the reverse-phase column. Calculating the extent of phosphorylation of T_{98} by integrating the peak areas under the triply charged ion for the unphosphorylated and phosphorylated peptide indicated an estimated stoichiometry of 44%, which agrees well with with the stoichiometry estimated for the endoproteinase LysC peptide K_{38} (42−48%).

The MS/MS spectra of T_{98} and phospho-T_{98} showed an abundant doubly charged y-ion series ranging from y_{12} to y_{22} (Figure 5 A,B). A fragment ion 33 Da smaller than the phosphorylated T_{98} precursor ion was observed, presumably from neutral loss of phosphoric acid (the mass of phosphoric acid is 98 Da; because the triply charged precursor ion was selected, loss of phosphoric acid produces an ion smaller by approximately 33 Da). This is often taken as proof that a peptide is phosphorylated (*41*). The fact that $y_{12}-y_{22}$ of phospho-T_{98} and of unphosphorylated T_{98} are identical immediately rules out Ser_{615} as the phosphate acceptor. The singly charged b_3-b_6 ions were observed in the spectrum of the nonphosphorylated peptide, whereas the corresponding b-ion series of the phospho-T_{98} was shifted by 80 Da starting from the b_2 ion (265.1 Da). Furthermore, as was already observed for the triply charged molecular ion, neutral loss of phosphoric acid was evident in the b-ion series: the phosphorylated b_4 ion (labeled with b_4*, Figure 5B) was

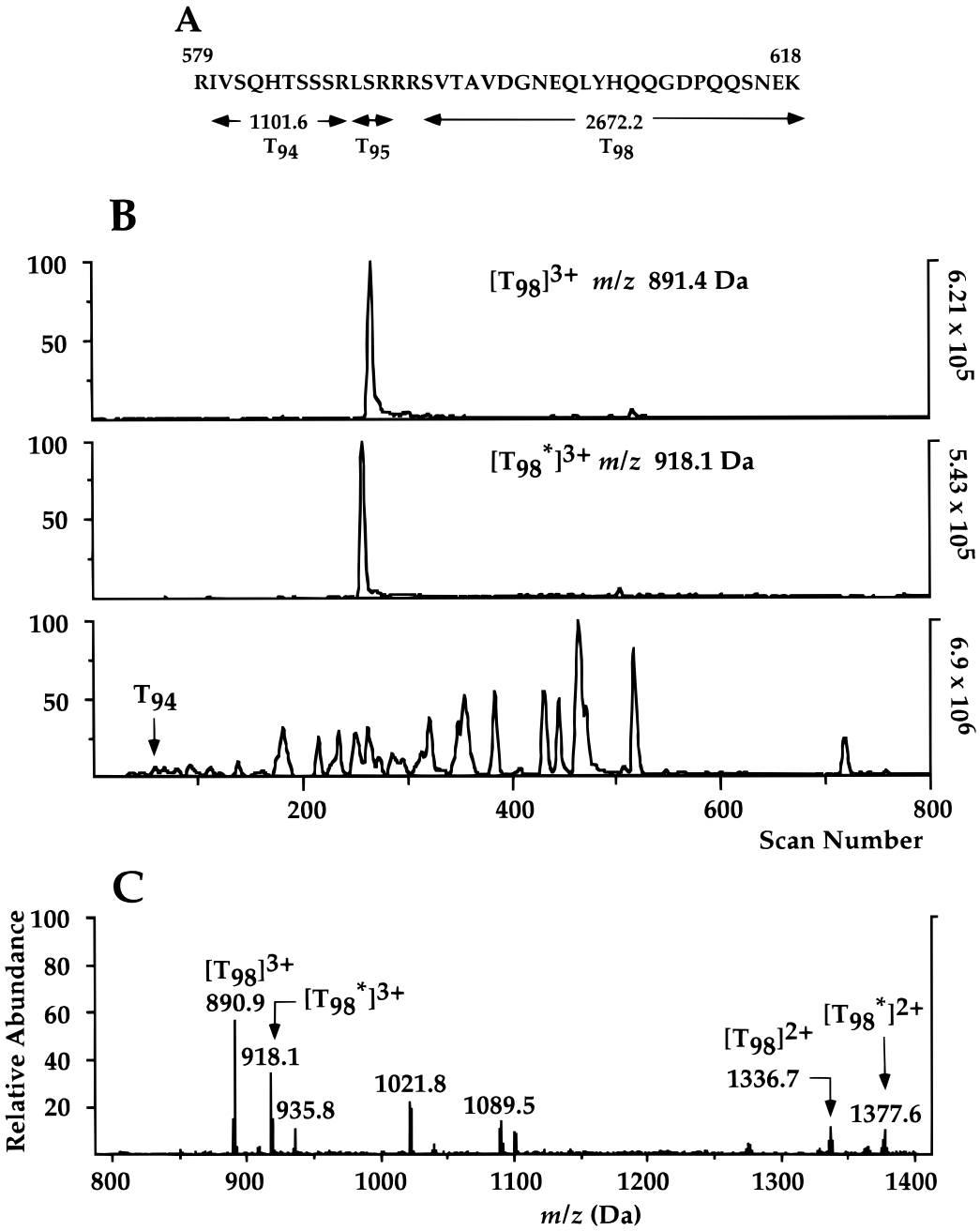

FIGURE 4: (A) Amino acid sequence, cleavage sites, and calculated masses (listed as singly protonated ions) of peptides produced by tryptic cleavage of the endoproteinase LysC peptide K_{38}. The residue numbers are indicated above the sequence. (B) Selected mass chromatograms for the triply charged T_{98} peptide (top panel) and the triply charged phospho-T_{98} peptide (middle panel) of an endoproteinase LysC/tryptic digest of interphase lamin. The bottom panel is the reconstructed ion current showing the sum of all ions present during the LC/MS run. Phospho-T_{98} elutes 10 scans earlier than the unphosphorylated T_{98} peptide during the LC/MS analysis. (C) Spectrum of the triply and doubly charged T_{98} and its phosphorylated form (labeled with an asterisk). The spectrum was generated by summing all scans acquired during the elution of T_{98} and phospho-T_{98}.

accompanied by a fragment ion 98 Da smaller (labeled with b_4^{Δ}, Figure 5B). The fact that b_2 had an observed mass 80 Da higher than its nonphosphorylated counterpart indicates that Ser_{595} is a site of phosphorylation in interphase lamin (Figure 5C).

Analysis of Phosphopeptide K_2 from Interphase and M-Phase Lamin. K_2 was also too large to obtain useful MS/MS data. Smaller peptides were obtained by digesting K_2 with clostripain. From the expected six cleavage products of K_2, doubly and triply charged ions of the two CP_3 and CP_4 peptides were detected (Figure 6). Inspection of the spectra of CP_3 and CP_4 revealed that no phosphate was associated with CP_3, whereas the spectrum of the triply and doubly charged ions of CP_4 showed ions 27 and 40 Da larger than for the unphosphorylated peptide, respectively. Furthermore, the intensities of the triply charged phospho-CP_4 ions and of the unphosphorylated CP_4 ions closely parallel the stoichiometry of phosphorylation observed in K_2 isolated from interphase lamin, ruling out the possibility that minor phosphorylation sites were overlooked which would reside on CP_3 (Figure 6 D).

MS/MS spectra of unphosphorylated and phosphorylated forms of CP_4 from interphase lamin show an identical set of unphosphorylated fragment ions, whose masses correspond

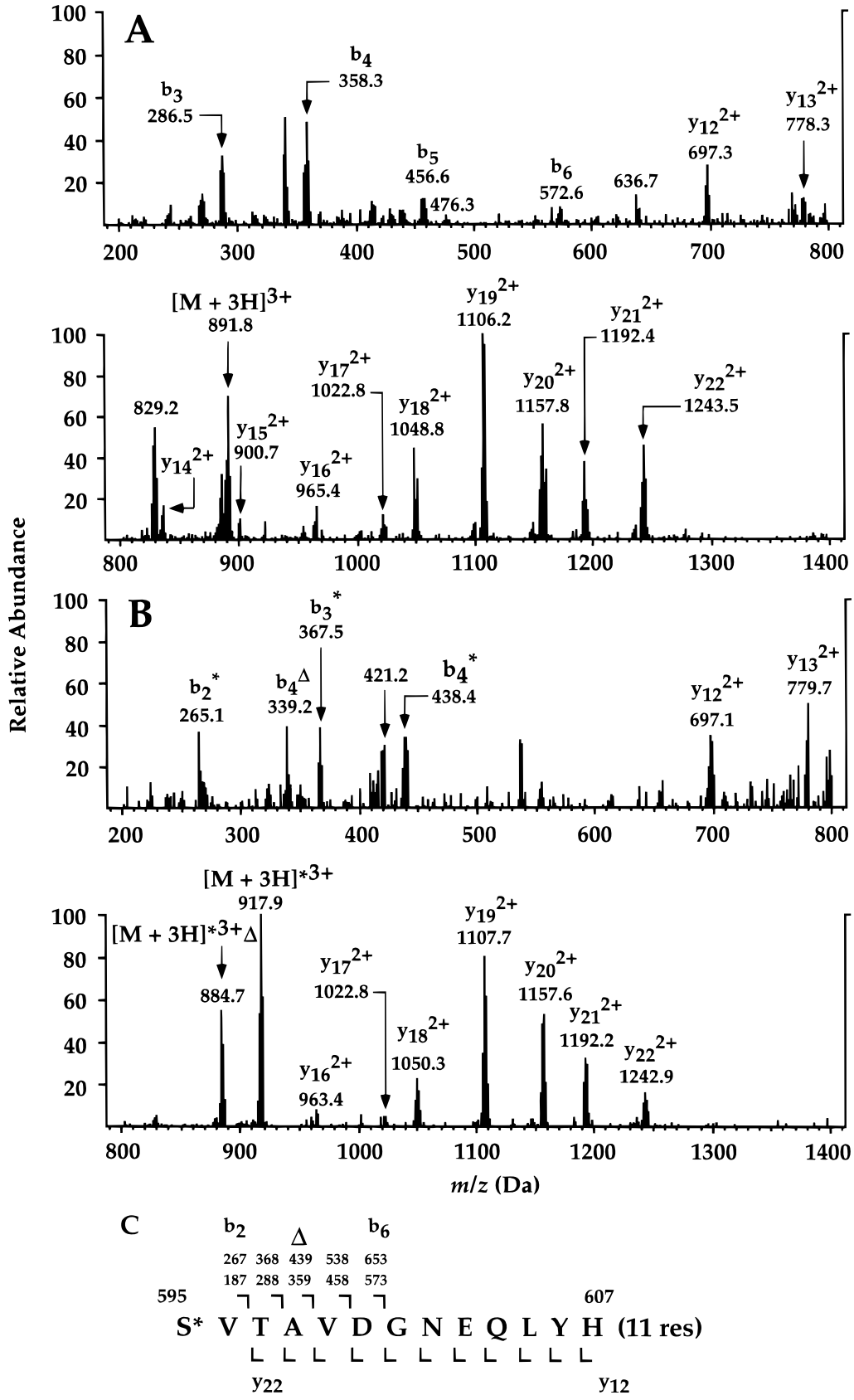

FIGURE 5: Comparison of the MS/MS spectra of T_{98} (A) and phospho-T_{98} (B) from interphase lamin. The triply charged precursor ion was selected for the collision experiments. Phosphorylated fragment ions are indicated by *, ions that have undergone neutral loss of phosphoric acid are indicated by Δ. To maximize signal intensity, quadrupole three in this experiment was set to transmit a mass window of approximately 3 Da. Therefore, the measured *m*/*z* values for the daughter ions can deviate from the predicted *m*/*z* values by up to 1.5 Da. (C) Summary of the observed b- and y-ions in the MS/MS spectra of T_{98}/phospho-T_{98}. Only the first 13 residues of the sequence of T_{98} which could be observed as y- or b-ions are shown, the remaining 11 amino acids are abbreviated with (11res). The predicted b-ions are listed above the sequence for unphosphorylated T_{98} (lower row) and for phospho-T_{98} (upper row) by assuming phosphorylation on the serine indicated with an asterisk (Ser_{595} in the amino acid sequence of *Drosophila* lamin).

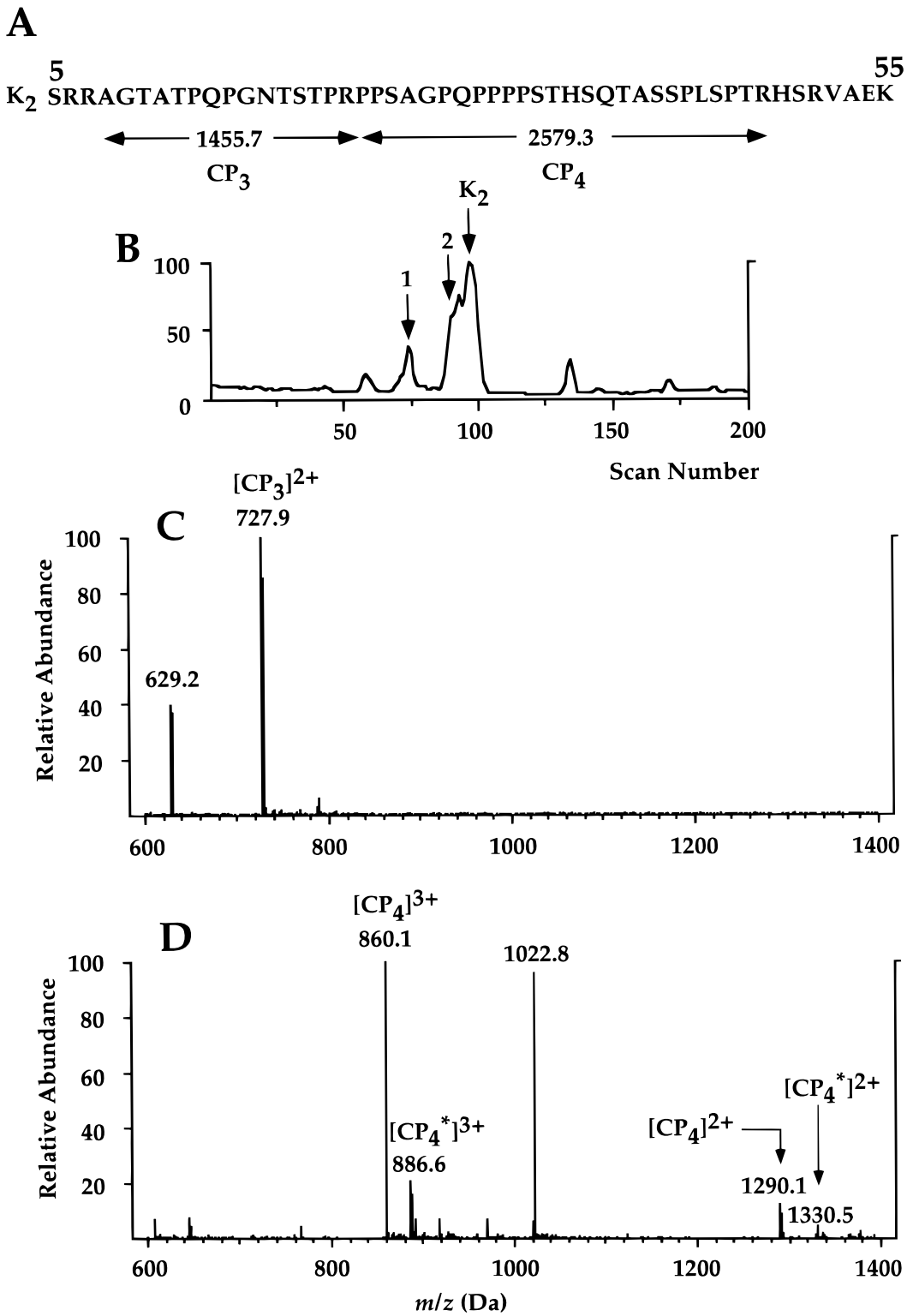

FIGURE 6: (A) Amino acid sequence, cleavage sites, and calculated masses (listed as singly protonated ions) of peptides produced by clostripain cleavage of the endoproteinase LysC peptide K_2. (B) Reconstructed ion current of the LC/MS analysis of the clostripain cleavage products of K_2 isolated from interphase lamin. The peaks labeled with 1 and 2 indicate the elution position of the CP_3 and CP_4 peptides. The peak labeled with K_2 is undigested peptide. (C) Mass spectrum of the peptide CP_3. (D) Mass spectrum of CP_4. The phosphorylated triply and doubly charged CP_4 peptides are labeled with an asterisk.

to those predicted for $y_{19}-y_6$ (Figure 7 A, B; note that only the *m*/*z* range up to 1400 Da, which covers the y-ion series up to y_{13}, is shown). This places the site of phosphorylation beyond y_{19} (corresponding to residues 23−29 of the lamin sequence). Because there is only one candidate serine remaining, it can be concluded that Ser_{25} of lamin is the phosphorylated residue. Positive identification of this site was seen in a set of ions, corresponding to b_2-b_7 where b_3-b_7 shifted by 80 Da in the phospho-CP_4 MS/MS spectrum compared with the nonphosphorylated CP_4, as well as the corresponding fragments resulting from neutral loss of phosphoric acid. These observations allow unambiguous identification of Ser_{25} as a phosphorylated residue in interphase lamin.

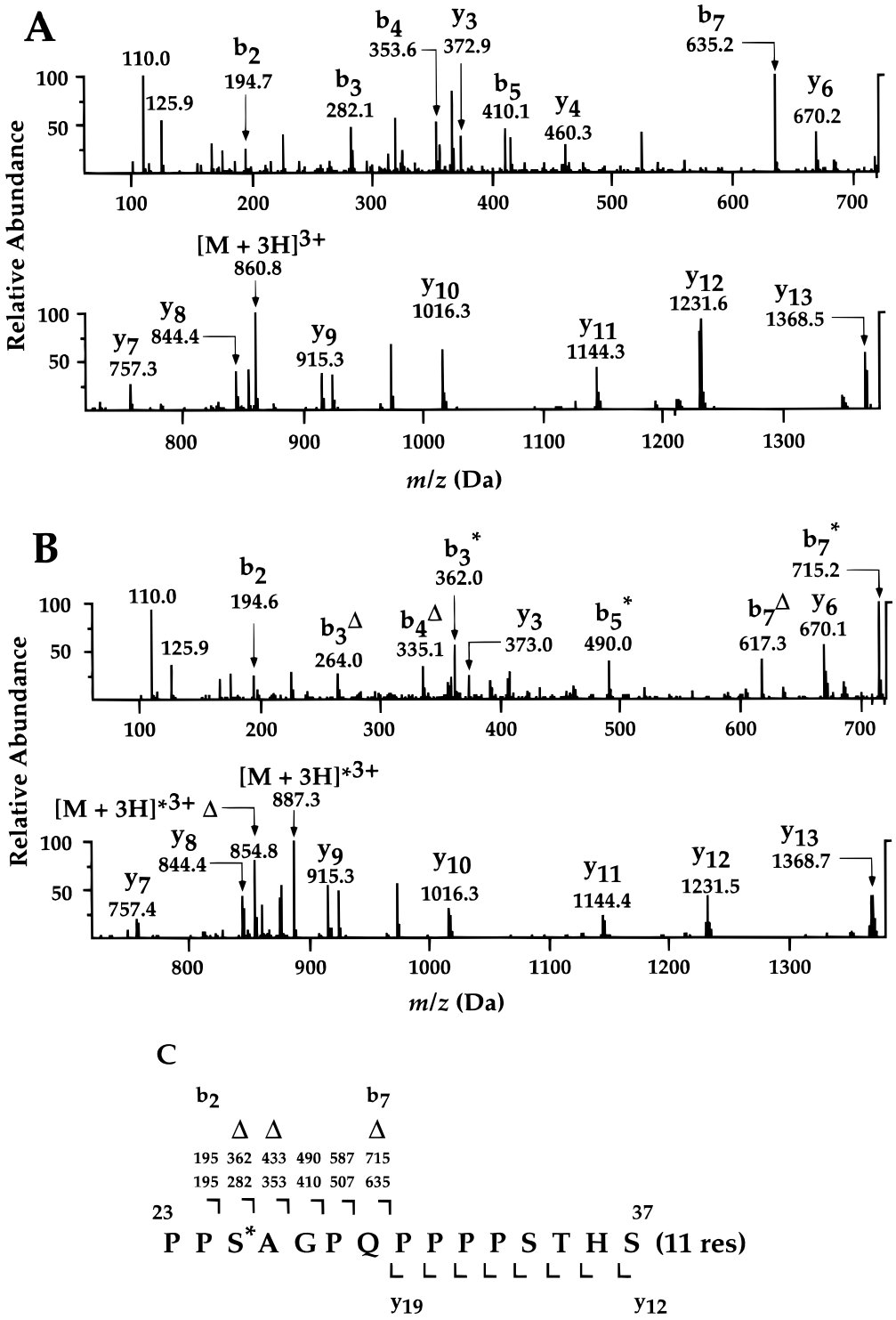

FIGURE 7: Comparison of the MS/MS spectra of (A) the unphosphorylated and (B) the phosphorylated CP_4 peptide from interphase lamin. In both experiments, the triply charged ion was selected for fragmentation. For reasons of clarity, only the *m*/*z* range between 100 and 1400 Da is shown. For labeling of the ions see Figure 5. (C) Summary of the observed b- and y-ions in the MS/MS spectrum of CP_4. The predicted b-ions are listed above the sequence for unphosphorylated CP_4 (lower row) and for phospho-CP_4 (upper row) by assuming phosphorylation on the serine indicated with an asterisk (Ser_{25} in the amino acid sequence of *Drosophila* lamin). Δ marks those ions that have undergone neutral loss of phosphoric acid during the collision process.

Phosphorylation of K_2 isolated from M-phase lamin was increased when compared to the same peptide isolated from interphase lamin. This could either mean that Ser_{25} is phosphorylated to a greater extent or that a site other than Ser_{25} is phosphorylated to higher stoichiometry. To distinguish between these two possibilities, phospho-CP_4 isolated from interphase or from M-phase lamin was subjected to fragmentation. Comparison of the fragmentation spectra reveals major differences between the two CP_4 peptides: most predominantly, 80 Da shifts due to the presence of a phosphorylated residue can be observed for $y_{10}-y_{18}$ in the spectrum of phospho-CP_4 derived from M-phase lamin, as well as fragments corresponding to y_6-y_{13} after neutral loss. The set of phosphorylated b fragment ions are also not

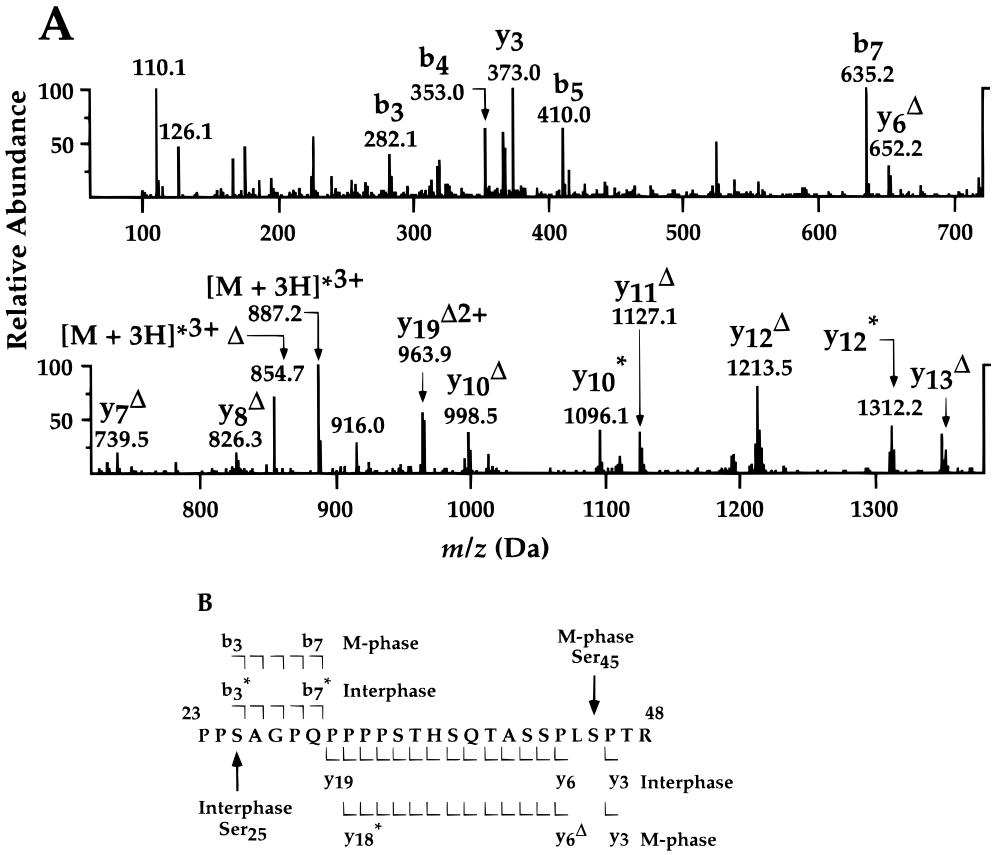

FIGURE 8: (A) MS/MS spectrum of the phosphorylated clostripain peptide CP_4 from M-phase lamin. The triply charged ion was selected for fragmentation. The corresponding MS/MS spectrum for the phosphorylated clostripain peptide CP_4 from interphase lamin is shown in Figure 7B. For labeling of the ions see Figure 5. (B) Summary of the observed b- and y-ions of the CP_4 fragment from interphase and M-phase lamin. The arrows indicate the site of phosphorylation which occurs on Ser_{25} during interphase and on Ser_{45} during M-phase.

observed in this case (Figure 8 A, B). This indicates that the site of phosphorylation of the head region in M-phase lamin has changed to a residue located C-terminal of Ser_{25}. Localization of the phosphorylated residue in the M-phase CP_4 fragment becomes evident upon inspection of the low mass range of the spectrum. In both phosphopeptides (interphase and M-phase forms) the y_3 ions are identical. This eliminates Thr_{47} as the site of phosphorylation. Localization of the phosphorylated residue in interphase CP_4 was possible due to the presence of the y_6 ion which underwent neutral loss of phosphoric acid (Figure 8 A, B). Because there is only one candidate serine within the ion series covered between y_3 and y_6, it can therefore be concluded that Ser_{45} is the site which becomes phosphorylated in M-phase lamin.

Analysis of Phosphopeptide K_{26} from Interphase Lamin. Despite numerous efforts, unambiguous localization of the site of phosphorylation in interphase K_{26} has not yet been possible. The amino acid sequence (Figure 9) makes the peptide especially refractory to mass spectrometric analysis: first, when K_{26} was subjected to fragmentation in the collision cell of the mass spectrometer, abundant y-ions were obtained which covered the N-terminal region of the peptide between residues 2 and 21 (corresponding to residues 403−423 of the lamin). No difference in the CID spectra was obtained between K_{26} and phospho-K_{26} (results not shown) which indicates that the site of phosphorylation must be located in the C-terminal half of the peptide. Because of the high number of basic amino acids in the peptide, no

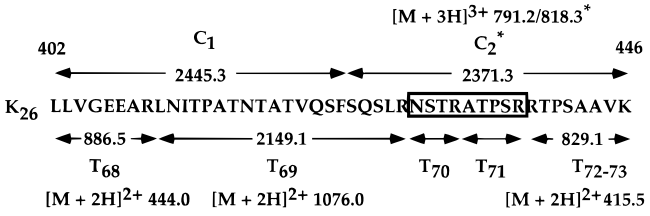

FIGURE 9: Amino acid sequence, cleavage sites, and calculated masses (listed as singly protonated ions) of peptides produced by chymotryptic or tryptic cleavage of the endoproteinase LysC peptide K_{26}. The peptides C_1 and C_2 generated upon chymotryptic cleavage are given above the sequence. The observed mass-to-charge ratios for C_2 were 791.2 Da for unphosphorylated and 818.3 Da for phosphorylated C_2, showing that the phosphate resides on the C-terminal half of K_{26}. The peptides and their calculated masses generated upon tryptic cleavage of K_{26} are given below the sequence (peptides T_{68}−T_{73}). Of the six expected peptides T_{68}, T_{69}, and the incompletely cleaved peptide T_{72-73} were observed. The two short peptides, T_{70} and T_{71}, could not be detected. No phosphate was found on tryptic peptides T_{69} or T_{72-73}. The boxed sequence denotes the presumed site of phosphorylation. For further details see the text.

substantial fragmentation covering the C-terminal half of K_{26} could be obtained. Upon chymotryptic cleavage of K_{26}, two peptides were observed whose masses indicated that the phosphate is associated exclusively with the C-terminal half of K_{26}. Neither the triply nor the quadruply charged chymotryptic peptides C_2 or phospho-C_2 (Figure 9) yielded any appreciable fragmentation in the collision cell of the mass spectrometer and could therefore not be exploited any further to localize the site of phosphorylation. Tryptic cleavage of

K_{26} should produce five peptides. Among these, T_{68} and T_{69} were found, whereas the C-terminal peptide was recovered as an incompletely cleaved peptide with the sequence RTPSAAVK. Inspection of the spectra showed no phosphate associated with either T_{69} or T_{72-73}, implying that the site of phosphorylation must reside on T_{70} or T_{71} (corresponding to residues 430−438 of lamin). The two tryptic peptides NSTR and ATPSR were not observed. Phosphoamino acid analysis of interphase lamin revealed the presence of both P-Ser and P-Thr (*42*). The two amino acids found to be phosphorylated in interphase lamin in the present study are serines. It is therefore tempting to say that the remaining phosphorylation site is either Thr_{432} or Thr_{435}. Nevertheless, final elucidation of the phosphorylation site on K_{26} has to await alternative analysis methods.

DISCUSSION

We analyzed the phosphorylation state of three lamin isoforms that can be isolated in relatively large quantities from *Drosophila* embryos. A soluble M-phase lamin was found to be phosphorylated predominantly at Ser_{45} (with a stoichiometry of about 0.75 mol phosphate/mol protein). Polymerized forms, called lamins Dm_1 and Dm_2, or interphase lamins, were phosphorylated in vivo at three residues: Ser_{25} in the N-terminal head domain (about 0.3 mol phosphate/mol protein), Ser_{595} in the C-terminal end of the C-terminal tail domain (about 0.5 phosphate/mol protein), and a third site (with about 0.2 phosphate/mol protein) between the α-helical rod domain and the nuclear localization signal which is probably either Thr_{432} or Thr_{435}.

Interphase form lamin Dm_2 (migrating on SDS-polyacrylamide gels slightly slower than lamin Dm_1) arises by differential phosphorylation as shown by treatment with alkaline phosphatase (*42*). Previously, mapping of the epitope of monoclonal antibody ADL84 (which binds lamin Dm_1 but not lamin Dm_2) to lamin residues 22−28 suggested the Dm_2-specific phosphorylation site to be Ser_{25} (*36*). Here, we demonstrate directly that Ser_{25} is indeed phosphorylated. As predicted, the stoichiometry of phosphorylation (about 0.3 phosphate/Ser_{25}) is similar to the ratio of lamin $Dm_2/(Dm_1 + Dm_2)$ in purified interphase lamins (about 0.3). This ratio is substantially higher in *Drosophila* embryos that were denatured immediately and analyzed by Western blotting using lamin-specific antibodies (N.S. unpublished observations), suggesting that some phosphatase activity (presumably nonspecific) lowered the phosphorylation stoichiometry during lamin purification.

M-phase lamin migrates on SDS-polyacrylamide gels at a position intermediate between those of lamins Dm_1 and Dm_2 (*34*). Apparently, phosphorylation of Ser_{45} (in M-phase lamin) slows migration in this gel system, and the lamin Dm_2-specific phosphorylation of Ser_{25} slows migration further (*36*). Another lamin isoform, named $Dm_{mit\text{-}s}$, that migrates even slower than lamin Dm_2 on SDS-polyacrylamide gels, arises both in vivo and when embryo nuclei are incubated in extracts made from stage 14 *Drosophila* oocytes (*43*). Antibody ADL84 does not bind to $Dm_{mit\text{-}s}$. In light of our current data, it seems likely that lamin $Dm_{mit\text{-}s}$ is phosphorylated on both Ser_{25} and Ser_{45}.

Two of the three interphase phosphorylation sites, Ser_{25} and Ser_{595}, do not have obvious homologues in vertebrate lamins. The *Drosophila* lamin head domain is significantly longer than the head domain of vertebrate lamins, and Ser_{25} and its surrounding residues do not have an apparent counterpart in any of the known vertebrate (or invertebrate) lamins, suggesting that whatever the function of phosphorylation of Ser_{25}, it is not widely conserved. It was previously shown that cAMP-dependent protein kinase (PKA) has a K_m for *Drosophila* lamin Dm_0 of <1 μM and that this low K_m is due almost exclusively to a C-terminal site (*44*). Our current data suggests that this site is Ser_{595}. In vivo, therefore, it is likely that Ser_{595} is modified by a PKA-like enzyme. The proximity of Ser_{595} to the C-terminus, which is implicated in attaching lamin to the inner nuclear membrane, further suggests that phosphorylation of this site might modulate membrane binding.

The third interphase site, most likely residing between amino acids 430 and 438, is located 19−29 residues C-terminal from the end of the lamin rod domain, preceding the nuclear localization signal. Again, no clear sequence homology with vertebrate lamins is found in this segment. However, all lamins known to date contain a high percentage of phosphorylatable residues between the end of the rod domain and the nuclear localization signal (see Figure 10). Indeed, many lamins are phosphorylated during interphase at one or more sites in this segment, and these phosphorylation events are carried out by several different kinases (depending on the organism and/or cell type in which the experiments were carried out, see Figure 10). Phosphorylation by PKC of two residues in chicken lamin B2 in the same lamin segment, located close to the nuclear localization signal (Ser_{410} and Ser_{411}), inhibits nuclear import of lamin B2 (*28*). It seems unlikely that phosphorylation of one of the candidate residues in the region between amino acids 430 and 438 of *Drosophila* lamin Dm_0 serves the same function because the interphase lamin analyzed here was purified from isolated nuclei and phosphorylation was catalyzed by a nuclear protein kinase (*42*). Therefore, intranuclear lamin was modified at this residue.

Our data show that the soluble (M-phase) lamin purified from early (0−4 h old) embryos is phosphorylated predominantly at Ser_{45}. This serine residue is found in a motif (SPTR) that matches the cdc2 kinase consensus recognition site (T/S PX K/R), and it was previously shown that Ser_{45} (and/or Ser_{42}) can be phosphorylated by cdc2 kinase in vitro (*44*). Other proline directed kinases have consensus sequences that also match this site. Indeed, it has been shown that two distinct MAP kinases phosphorylate chicken lamin B2 in vitro (*45*). All lamins known to date (except for the lamin from *Caenorhabditis elegans*) carry sites that are predicted to be phosphorylated by cdc2 kinase (as well as other proline directed kinases) and that are symmetrically positioned near the ends of the coiled-coil rod domain. A substantial amount of data indicates that phosphorylation of one or two of these sites is instrumental for disassembly of the nuclear lamina during mitosis (*17*, *18*, *20*, *21*, *23*, *45*). In agreement with the assumption that cdc2 kinase is responsible for phosphorylation of M-phase lamin, *Drosophila* cdc2 kinase (*46*) and several cdc2 kinase-related enzymes (*47*, *48*) are expressed and active (*49*, *50*) in preblastoderm embryos. Thus, phosphorylation of *Drosophila* lamin by cdc2 kinase appears to be instrumental for maintaining the maternally provided lamin in a soluble, M-phase, state.

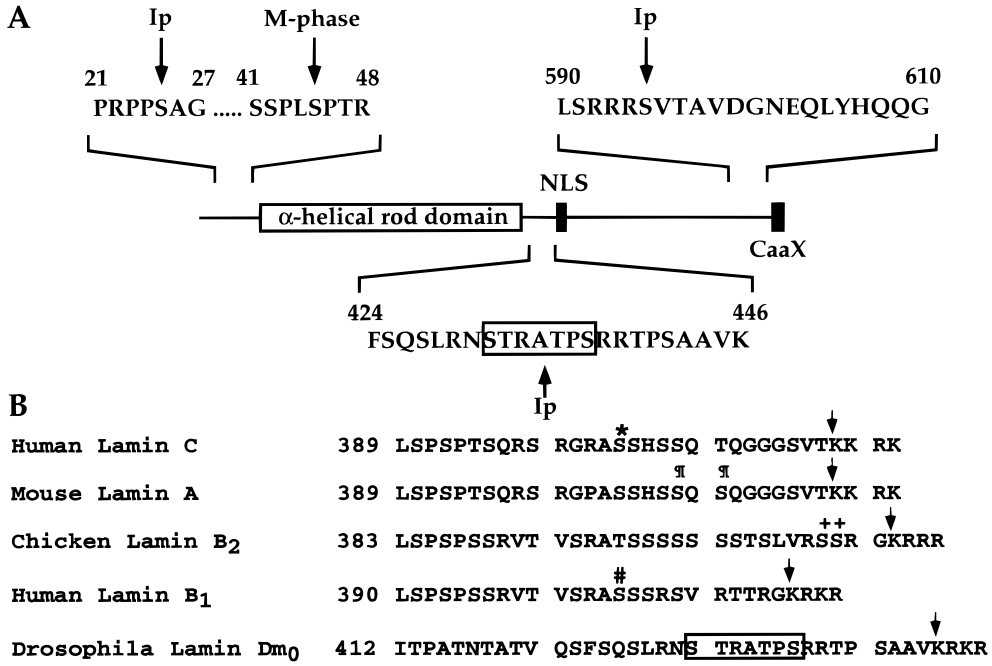

FIGURE 10: (A) Sites of phosphorylation in *Drosophila* lamin. The phosphorylated residues occurring in interphase and M-phase lamin are marked with Ip and M-phase, respectively. The sequence surrounded by a box marks the region of the presumed site of phosphorylation of K_{26}. (B) Comparison of phosphorylation sites from vertebrate and *Drosophila* lamins located in the region between the end of the α-helical rod domain and the nuclear localization signal (NLS). Sequences were placed such that the ends of the rod segments are aligned. For each partial lamin sequence, the downpointing arrow (↓) designates what is thought to be the start of the NLS. The Ser in human lamin C (labeled with *) was found to be phosphorylated with a *Xenopus laevis* oocyte extract (*19*), the two Ser in murine lamin A (labeled with ¶) were found to be phosphorylated during interphase in vivo (*23*, *51*), the two Ser labeled with ++ were found to inhibit nuclear import when phosphorylated (*28*), and the Ser labeled with # was shown to be a mitosis-specific site and was also found to be phosphorylated by PKC in vitro (*25*). See also text for more details.

Can the results presented here be extrapolated to the phosphorylation state of lamin Dm_0 derivatives in cells other than the embryonal cells used for lamin purification? It was previously suggested that lamin purified from M-phase *Drosophila* tissue culture cells is similar to the soluble lamin from the 0−4 h embryos (*34*) used in this study. This has been demonstrated in several contexts (P. F., unpublished). Comparison of our data with CNBr peptide maps of in vivo ^{32}P-labeled M-phase and interphase lamins purified from tissue culture cells (*34*) shows that both sets of data are compatible. However, the relevant CNBr fragments are relatively large (about 17 kDa), and two of the important peptides comigrate, precluding definite conclusions about the relation between lamin phosphorylation sites in tissue culture cells and embryos. Nevertheless, it can be concluded that, in tissue culture cells, the conversion of interphase lamin into M-phase lamin is accompanied by dephosphorylation of interphase sites (and phosphorylation of other, M-phase sites). It is worth mentioning that the sensitivity of mass spectral analysis of phosphorylation sites is certainly sufficient for a detailed mapping of the phosphorylation state of lamin isolated from tissue culture cells at various stages of the cell cycle.

Fields and co-workers demonstrated that M-phase human lamin B_1 isolated from K562 or HL60 cells (both are representatives of the erythroid cell lineage) is phosphorylated at three sites, one of which can also be phosphorylated by β_{II} PKC in vitro (*25*). This PKC site is located between the C-terminal end of the lamin rod domain and the nuclear localization signal. Likewise, solubilization of sea urchin lamin B incubated in G_1 phase sea urchin oocyte cytosol results from lamin phosphorylation by PKC (*27*). Inhibition of head-to-tail assembly of *Drosophila* lamin in vitro can result not only from phosphorylation of Ser_{45} by cdc2 kinase but also from phosphorylation of Ser_{50} (*44*). Taken together, these results show that disassembly of lamin polymers can be achieved through phosphorylation of a number of sites, all in close proximity to the coiled-coil rod domain, by different kinases. Although cdc2 kinase appears to be the most widely employed kinase, it is possible that the exact mechanism of lamin disassembly, including the kinases involved, is cell type-specific.

ACKNOWLEDGMENT

We thank Dr. C. Iden for critical reading of the manuscript.

REFERENCES

1. Gotta, M., and Gasser, S. M. (1996) *Experientia 52*, 1136−1147.
2. Fuchs, E., and Weber, K. (1994) *Annu. Rev. Biochem. 63*, 345−382.
3. Aebi, U., Cohn, J., Buhle, L., and Gerace, L. (1986) *Nature 323*, 560−564.
4. Bridger, J. M., Kill, I. R., O'Farrell, M., and Hutchison, C. J. (1993) *J. Cell Sci. 104*, 297−306.
5. Moir, R. D., Montag-Lowy, M., and Goldman, R. D. (1994) *J. Cell Biol. 125*, 1201−1212.
6. Newport, J. W., Wilson, K. L., and Dunphy, W. G. (1990) *J. Cell Biol. 111*, 2247−2259.
7. Ris, H. (1997) *Scanning 19*, 368−375.
8. Höger, T. H., Krohne, G., and Kleinschmidt, J. A. (1991) *Exp. Cell Res. 197*, 280−289.
9. Ludérus, M. E. E., den Blaauwen, J. L., de Smit, O. J. B., Compton, D. A., and van Driel, R. (1994) *Mol. Cell. Biol. 14*, 6297−6305.

10. Taniura, H., Glass, C., and Gerace, L. (1995) *J. Cell Biol. 131,* 33−44.
11. Moir, R. D., Spann, T. P., and Goldman, R. D. (1995) in *Structural and functional organization of the nuclear matrix* (Berezney, R., and Jeon, K. W., eds.), Vol. 162B, pp 141−182, Academic Press, Inc., San Diego.
12. McKeon, F. D. (1991) *Curr. Opin. Cell Biol. 3,* 82−86.
13. Heitlinger, E., Peter, M., Häner, M., Lustig, A., Aebi, U., and Nigg, E. A. (1991) *J. Cell Biol. 113,* 485−495.
14. Gieffers, C., and Krohne, G. (1991) *Eur. J. Cell Biol. 55,* 191−199.
15. Gerace, L., and Blobel, G. (1980) *Cell 19,* 277−287.
16. Ottaviano, Y., and Gerace, L. (1985) *J. Biol. Chem. 260,* 624−632.
17. Heald, R., and McKeon, F. (1990) *Cell 61,* 579−589.
18. Peter, M., Nakagawa, J., Doree, M., Labbe, J. C., and Nigg, E. A. (1990) *Cell 61,* 591−602.
19. Ward, G. E., and Kirschner, M. W. (1990) *Cell 61,* 561−577.
20. Dessev, G., Iovcheva-Dessev, C., Bischoff, J. R., Beach, D., and Goldman, R. (1991) *J. Cell Biol. 112,* 523−533.
21. Peter, M., Heitlinger, E., Häner, M., Aebi, U., and Nigg, E. A. (1991) *EMBO J. 10,* 1535−1544.
22. Nigg, E. A. (1992) *Curr. Opin. Cell Biol. 4,* 105−109.
23. Eggert, M., Radomski, N., Linder, D., Tripier, D., Traub, P., and Jost, E. (1993) *Eur. J. Biochem. 213,* 659−671.
24. Hocevar, B. A., Burns, D. J., and Fields, A. P. (1993) *J. Biol. Chem. 268,* 7545−7552.
25. Goss, V. L., Hocevar, B. A., Thompson, L. J., Stratton, C. A., Burns, D. J., and Fields, A. P. (1994) *J. Biol. Chem. 269,* 19074−19080.
26. Thompson, L. J., and Fields, A. P. (1996) *J. Biol. Chem. 271,* 15045−15053.
27. Collas, P., Thompson, L., Fields, A. P., Poccia, D. L., and Courvalin, J. C. (1997) *J. Biol. Chem. 272,* 21274−21280.
28. Hennekes, H., Peter, M., Weber, K., and Nigg, E. A. (1993) *J. Cell Biol. 120,* 1293−1304.
29. Kill, I. R., and Hutchison, C. J. (1995) *FEBS Lett. 377,* 26−30.
30. Bossie, C. A., and Sanders, M. M. (1993) *J. Cell Sci. 104,* 1263−1272.
31. Whalen, A. M., McConnell, M., and Fisher, P. A. (1991) *J. Cell Biol. 112,* 203-213.
32. Riemer, D., Stuurman, N., Berrios, M., Hunter, C., Fisher, P. A., and Weber, K. (1995) *J. Cell Sci. 108,* 3189−3198.
33. Ashery-Padan, R., Ulitzur, N., Arbel, A., Goldberg, M., Weiss, A. M., Maus, N., Fisher, P. A., and Gruenbaum, Y. (1997) *Mol. Cell. Biol. 17,* 4114−4123.
34. Smith, D. E., and Fisher, P. A. (1989) *J. Cell Biol. 108,* 255−265.
35. Lin, L., and Fisher, P. A. (1990) *J. Biol. Chem. 265,* 12596−12601.
36. Stuurman, N., Maus, N., and Fisher, P. A. (1995) *J. Cell Sci. 108,* 3137−3144.
37. Gilles, A.-M., Imhoff, J.-M., and Keil, B. (1979) *J. Biol. Chem. 154,* 1462−1468.
38. Gruenbaum, Y., Landesman, Y., Drees, B., Bare, J. W., Saumweber, H., Paddy, M. R., Sedat, J. W., Smith, D. E., Benton, B. M., and Fisher, P. A. (1988) *J. Cell Biol. 106,* 585−596.
39. Davis, M. T., and Lee, T. D. (1995) *Anal. Chem. 67,* 4549−4556.
40. Carr, S. A., Huddleston, M. J., and Annan, R. S. (1996) *Anal. Biochem. 239,* 180−192.
41. Payne, M. D., Rossomando, A. J., Martino, P., Erickson, A. K., Her, J.-H., Shabanowitz, J., Hunt, D. F., Weber, M. J., and Sturgill, T. W. (1991) *EMBO J. 10,* 885−892.
42. Smith, D. E., Gruenbaum, Y., Berrios, M., and Fisher, P. A. (1987) *J. Cell Biol. 105,* 771−790.
43. Maus, N., Stuurman, N., and Fisher, P. A. (1995) *J. Cell Sci. 108,* 2027−2035.
44. Stuurman, N. (1997) *FEBS Lett. 401,* 171−174.
45. Peter, M., Sanghera, J. S., Pelech, S. L., and Nigg, E. A. (1992) *Eur. J. Biochem. 205,* 287−294.
46. Lehner, C. F., and O'Farrell, P. H. (1990) *EMBO J. 9,* 3573−3581.
47. Stern, B., Ried, G., Clegg, N. J., Grigliatti, T. A., and Lehner, C. F. (1993) *Development 117,* 219−232.
48. Sauer, K., Weigmann, K., Sigrist, S., and Lehner, C. F. (1996) *Mol. Biol. Cell 7,* 1759−1769.
49. Edgar, B. A., Sprenger, F., Duronio, R. J., Leopold, P., and O'Farrell, P. H. (1994) *Genes Dev. 8,* 440−452.
50. Lee, K. S., Yuan, Y. L., Kuriyama, R., and Erikson, R. L. (1995) *Mol. Cell. Biol 15,* 7143−7151.
51. Eggert, M., Radomski, N., Tripier, D., Traub, P., and Jost, E. (1991) *FEBS Lett. 292,* 205−209.

BI9827060